

Effect of Nitriding Treatment on Fatigue life for Free Piston Linear Engine Component using Frequency Response Method: a Finite Element Approach

M. M. Rahman¹, A. K. Ariffin², S. Abdullah² and A. B. Rosli¹

Abstract: Low weight and long lifetime are necessary requirements for automobiles to significantly reduce CO₂ emission and environmental burdens in their use. Aluminum alloys are one of the most promising materials selections for automobiles parts and electrical components to reduce their weight and to increase their specific strength. This paper presents the role of nitriding on the fatigue life of the vibrating cylinder block for a new two-stroke free piston engine using variable amplitude loading conditions. The finite element modeling and analysis have been performed utilising a computer aided design and a finite element analysis codes respectively. In addition, the fatigue life prediction was carried out using finite element based fatigue analysis code. The material AA6061-T6 is considered in this study. The narrow band frequency response approach was applied to predict the fatigue life of cylinder block using different load histories. Based on the finite element results, it is observed that there is a significant variation between the nitriding treatment and untreated cylinder block of free piston engine. The obtained results indicate that the nitrided treatment produces longest life for all loading conditions. Therefore, the nitriding process is one of the promising surface treatments for aluminum alloy parts to increase the fatigue life of the linear engine cylinder block.

Keyword: Finite element method, free piston engine, cylinder block, fatigue life, nitriding, narrow band frequency response.

1 Introduction

Light metals have been utilized for automotive parts to reduce the weight of automobiles, aiming at the significant reduction of CO₂ emission and environmental burdens [Boms and Whitacre (2005); Vissutipitukul and Aizawa (2005)]. The use of aluminum (Al) instead of steel for lightening of vehicle components or machine parts has recently increased. Al and its alloys have advantages over non metallic materials: aluminum alloys have a high melting point, a good corrosion resistant, a good workability and have a good thermal conductivity. However, the hardness and wear resistance of Al alloys are respectively lower and inferior to those of steel; therefore, there is a limit in their application to moving parts. Hence, research has been carried out in surface modification technology to increase the applicability of Al alloys as moving parts. Surface modification technologies for Al alloys can be classified into three main groups. Alloying is the first method and this forms a hard film on the Al surface [Tomida and Nakata (2003); Okumiya et al. (2005)]. The second group is coating method, which covers the Al surface with hard materials [Tsunekawa et al. (2003); Takeuchi et al. (2004)]. The third is a heat treating process, such as nitriding [Okumiya et al. (2001)]. Nitriding is now widely used in manufacturing for surface hardening of ferrous and non-ferrous materials. Nitriding, one of the most widely used thermo-chemical methods, produces a high compressive residual stresses on the surfaces of components. Nitriding is a process for hardening the surface by diffusing nitrogen into the surface. Nitriding processes are performed at temperatures between 500°C and 550°C where the structure is still ferritic.

The control of failures due to the high cycle fa-

¹ Faculty of Mechanical Engineering, Universiti Malaysia Pahang, P. O. Box 12, 25000 Kuantan, Pahang, Malaysia. Phone: +(6)-09-5492207, Fax: +(6)-09-5492244, E-mail: mustafizur@ump.edu.my

² Department of Mechanical and Materials Engineering, Universiti Kebangsaan Malaysia, 43600 UKM, Bangi, Selangor DE, Malaysia

tigue (HCF) in the two-stroke free piston engine components is one of the most critical challenges [Bell et al. (1998)]. Fatigue is an important parameter to be considered in the behaviour of components subjected to complex random loading [Torres and Voorwald (2002)]. Fatigue is of great concern for components subject to cyclic stresses, particularly where safety is paramount, for examples free piston linear generator engine components [Rahman and Ariffin (2006)]. It has long been recognized that fatigue cracks generally initiate from free surfaces and that performance is therefore reliant on the surface topology/integrity produced by surface finishing.

The objective of the current study is specifically to investigate into the effect of nitriding treatments on the fatigue life improvement of the cylinder block of linear engine. Numerical investigations are performed to characterize completely the different induced effects before and after nitriding surface treatments. The numerical results were discussed and analysed. Their influences on HCF behaviour of the vibrating component made from AA 6061-T6. However, these investigations are essential in order to understand the involved microstructural mechanisms of hardening or softening in the wake of service load.

2 Theoretical Basis

The stress power spectra density represents the frequency domain approach input into the fatigue [Bishop and Sherratt (2000)]. This is a scalar function that describes how the power of the time signal is distributed among frequencies [Bendat (1964)]. Mathematically this function can be obtained by using a Fourier Transform of the stress time history's auto-correlation function, and its area represents the signal's standard deviation. It is clear that PSD is the most complete and concise representation of a random process.

The most convenient way of storing stress range histogram information is in the form of a probability density function (PDF) of stress ranges [Bendat (1964); Rahman (2007)]. A typical representation of this function is shown in Fig. 1. It is easily to transform from a stress range histogram to a PDF, or back to time histories. The bin widths

used and the total number of cycles recorded in the histogram are the only additional information required. To get a PDF from a rainflow histogram each bin in the rainflow count has to be multiplied by $S_i \times dS$, where S_i is the total number of cycles in histogram and dS is the interval width. The probability of the stress range occurring between $S_i - dS/2$ and $S_i + dS/2$ is given by $p(S_i)dS$. The actual counted number of cycles, $n_i = p(S)dSS_i$. The allowable number of cycles, $N(S_i) = \frac{k}{S_i^b}$.

Then damage is defined as,

$$E[D] = \sum_i \frac{n_i}{N(S_i)} = \frac{S_t}{k} \int S^b p(S) dS \quad (1)$$

Failure occurs, $D \geq 1.0$.

In order to compute fatigue damage over the lifetime of the structure in seconds the form of materials $S - N$ data must also be defined using the material parameters k and b .

The typical $S - N$ curve for high cycle fatigue is as shown in Fig. 2. This figure simply shows that, under constant amplitude cyclic loading, a linear relationship exists between cycles to failure (N) and applied stress range (S) when plotted on log-log paper. There are two alternative ways of defining this relationship, as given in Eq. (2).

$$N = kS^{-b}, \quad (2)$$

where $b = -\frac{1}{b_1}$, and $k = (SRI1)^{b_1}$.

A method for computing PSD moments is described by Rahman (2007). Some very important statistical parameters can be computed from these moments. These parameters are root mean square (RMS), number of Zero crossing with positive slope ($E[0]$), number of peaks per second ($E[P]$). The formulas in Eq. (3) highlight these properties of the spectral moments.

$$RMS = \sqrt{m_0}; \quad E[0] = \sqrt{\frac{m_2}{m_0}}; \quad E[P] = \sqrt{\frac{m_4}{m_2}} \quad (3)$$

where m_0, m_1, m_2 , and m_4 are the zero, 1st, 2nd and 4th order moment of area of the PSD respectively.

Another important property of spectral moments is the fact that it is possible to express the irregularity factor as a function of the zero, second and

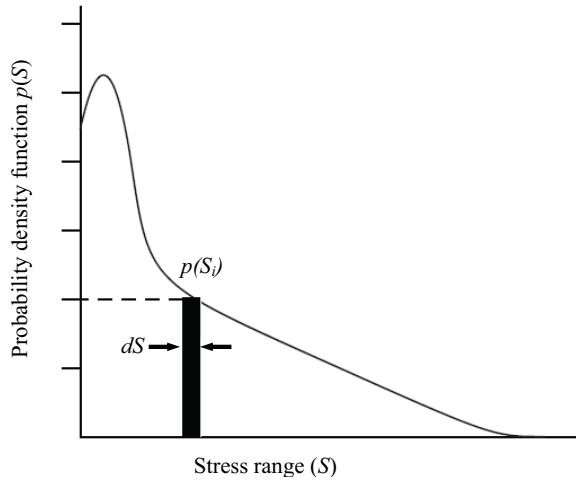


Figure 1: Probability density functions

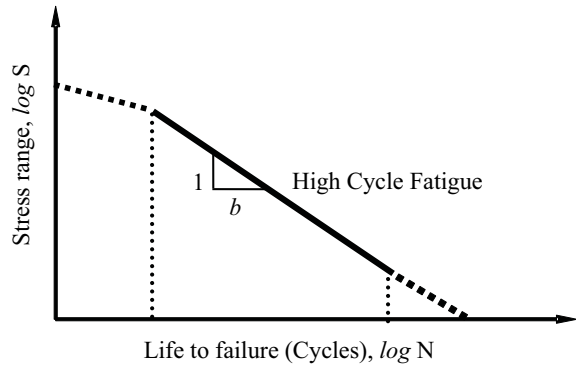


Figure 2: Typical $S - N$ curve for high cycle fatigue [Bishop and Sherratt (2000)]

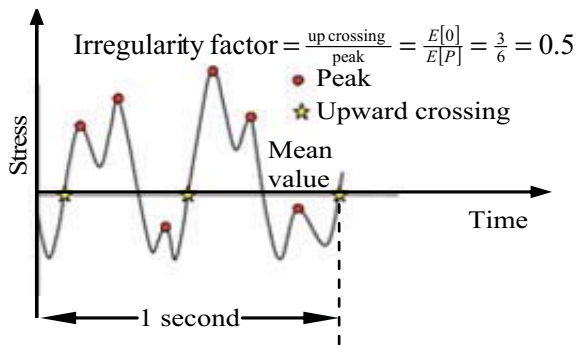


Figure 3: Calculation of the irregular factor, γ

fourth order spectral moments, as shown in Eq. (4).

$$\gamma = \frac{E[0]}{E[P]} = \frac{m_2}{\sqrt{m_0 m_4}} \quad (4)$$

Fig. 3 shows how to calculate the irregular factor

tor. When irregularity factor is equal to 0, there are an infinite number of peaks for every zero upcrossing. This is considered a wide band random process. The value of irregularity factor is equal to 1 corresponds to one peak per one zero upcrossing and it represents a narrow-band random process. Alternatively, a narrow-band process can be defined by the width of its spectrum. For this reason, the spectral width parameter, λ , is introduced as

$$\lambda = \sqrt{1 - \gamma^2} \quad (5)$$

That means $\lambda = 0$ represents a narrow-band random process.

The irregularity factor γ is an important parameter that can be used to evaluate the concentration of the process near a central frequency. Therefore, the irregularity factor can be used to determine whether the process is narrow band or wide band. Irregularity factor varies between 1 and 0. A narrow band process ($\gamma \rightarrow 1$) is characterized by only one predominant central frequency indicating that the number of peaks per second is very similar to the number of zero crossings of the signal. This assumption leads to the fact that the PDF of the fatigue cycles range is the same as the PDF of the peaks in the signal. In this case fatigue life is easy to estimate.

Bendat (1964) has proposed first significant step towards a method of determining fatigue life from PSDs. Bendat showed that the PDF of the peaks for a narrow band signal tended towards Rayleigh distributions as the bandwidth reduced. Furthermore, for a narrow band time history Bendat assumed that all the positive peaks in the time history would be followed by corresponding troughs of similar magnitude regardless of whether they actually formed stress cycles. Using this assumption, the PDF of stress range would also to a Rayleigh distribution. Bendat used a series of equations derived by Race (1954) to estimate the expected number of peaks using moments of area beneath the PSD.

Assume $p(S)$ is the Rayleigh distribution which is represented by a narrow band process and stress amplitude, S , can be treated as a continuous ran-

dom variable.

$$p(S)_{NB} = f(m_0) = \frac{S}{4m_0} e^{-\frac{S^2}{8m_0}} \quad (6)$$

The expected total fatigue damage for narrow band Gaussian process,

$$\begin{aligned} E[D] &= \sum_i \frac{n_i}{N(S_i)} = \frac{S_t}{K} \int S^b p(S) dS \\ &= \frac{E[P]T}{K} \int S^b \left[\frac{S}{4m_0} e^{-\frac{S^2}{8m_0}} \right] dS \quad (7) \end{aligned}$$

where $N(S_i)$ is the number of cycles of stress range S occurring in T seconds, n_i is the actual counted number of cycle, S_t is the total number of cycles equals to $E[P]T$.

Even though any statistical model of S can be employed, it is common to use the Weibull distribution

$$F(S) = 1 - e^{-\left(\frac{S}{\alpha}\right)^\beta} \quad (8)$$

where α and β are the scale parameter or characteristic life and shape parameter or Weibull slope respectively. For Weibull distribution

$$E(S^b) = \alpha^b \Gamma\left(\frac{b}{\beta} + 1\right) \quad (9)$$

where $\Gamma(\cdot)$ is the Gamma function.

The Weibull distribution reduces to Rayleigh distribution when $\beta = 2$. Rayleigh is the distribution of peaks or ranges or amplitudes in a stationary narrow band Gaussian process that has an RMS value.

$$\alpha = \sqrt{2}RMS = \sqrt{2m_0} \quad (10)$$

Therefore, we get solution from Eq. (9) is expressed in Eq. (11)

$$E(S^b) = \left(\sqrt{2m_0}\right)^b \Gamma\left(\frac{b}{\beta} + 1\right) \quad (11)$$

The expected total fatigue damage, $E[D]$, of the zero mean stationary narrow band Gaussian process over a time interval τ can be expressed as Eq. (12).

$$E[D] = \frac{E[P]T}{K} \left(\sqrt{2m_0}\right)^b \Gamma\left(\frac{b}{\beta} + 1\right) \quad (12)$$

This is the first frequency response method for predicting fatigue damage from PSDs and it assumes that the PDF of peaks is equal to the PDF of stress amplitudes. The narrow band solution was then obtained by substituting the Rayleigh PDF of peaks with the PDF of stress ranges. The full equation is obtained by noting that S_t is equal to $E[P].T$, where T is the life of the structure in seconds. The basis of the narrow band solution is shown in Fig. 4.

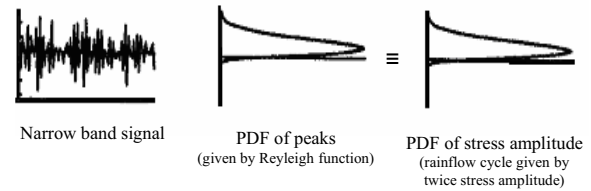


Figure 4: Basis of the narrow band solution [Bishop and Sherratt (2000)]

3 Results and Discussion

3.1 Finite Element Modeling and Analysis

A geometric model of the cylinder block of the free piston engine is considered in this study. Three-dimensional model geometry was developed in CATIA[®] software. Since the tetrahedral is found to be the best meshing technique, the 4 nodes tetrahedral (TET4) element version of the cylinder block was used for the initial analysis. In addition, the TET4 compared to the 10 nodes tetrahedral (TET10) element mesh using the same global mesh length for the highest loading conditions (7.0 MPa) in the combustion chamber. The investigating the results, it can be found that the TET10 mesh predicted higher von Mises stresses than that the TET4 mesh. The TET10 mesh is presumed to represent a more accurate solution since TET4 meshes are known to be dreadfully stiff [Felippa (2001)]. TET4 employed a linear order interpolation function while TET10 used quadratic order interpolation function. For the same element size, the TET10 is expected to be able to capture the high stress concentration associated with the bolt holes. A parabolic tetrahedral element (TET10) was then finally used for

the solid mesh. Mesh study is performed on the FE model to ensure sufficiently fine sizes are employed for accuracy of calculated results but at competitive cost (CPU time). In the process, specific field variable is selected and its convergence is monitored and evaluated. Sensitivity analysis was performed to obtain the optimum element size. The analysis was performed iteratively at different element lengths until the solution obtained appropriate accuracy. Convergence of the stresses was observed, as the mesh size was successively refined. The element size of 0.20 mm was finally considered. A total of 35415 elements and 66209 nodes were generated with 0.20 mm element length. Compressive loads were applied as pressure (7 MPa) acting on the surface of the combustion chamber and preloads were applied as pressure (0.3 MPa) acting on the bolt-hole surfaces. In addition, preload was also applied on the gasket surface generating pressure of 0.3 MPa. The loading and constraints on the cylinder block are shown in Fig. 5. The constraints were applied on the bolt-hole for all six degree of freedoms. Multi-point constraints (MPCs) [Schaeffer (2001)] were used to connect the parts through the interface nodes. These MPCs were acting as an artificial bolt and nut that connect each parts of the structure. Each MPC's will be connected using a Rigid Body Element (RBE) that indicating the independent and dependent nodes. The configuration of the engine is constrained by bolt at the cylinder head and cylinder block. In condition with no loading configuration the RBE element with six-degrees of freedom were assigned to the bolts and the head hole. The independent node was created on the cylinder block hole. The finite element analysis of the time domain histories is performed using the finite element software employed the linear static analysis method [Schaeffer (2001)].

The finite element results of time domain (Pseudo-static method) i.e. the maximum principal stresses distribution is presented in Fig. 6. The fatigue life of time domain histories are performed using the stress-life method employed rainflow cycle counting technique [Anthes (1997); Khosrovaneh and Downing (1990)].

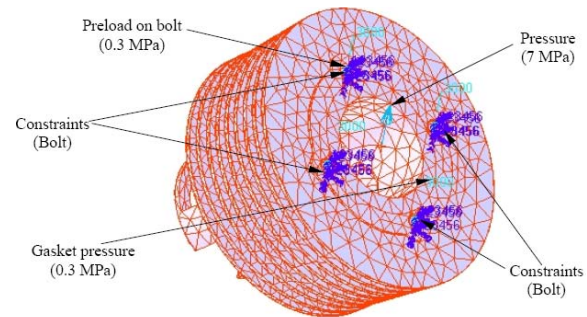


Figure 5: Loading and constraints on the cylinder block

Time domain fatigue approach consists of a number of steps. The first is to count the number of stress cycles in the response time history. This is performed through a process of rain flow cycle counting. Damage from each cycle is determined, typically from an $S - N$ curve. The damage is then summed over all cycles using linear damage summation techniques to determine the total life. The frequency response analyses were performed using the finite element analysis code. The frequency response analysis used the damping ratio of 5% of critical. The damping ratio is the ratio of the actual damping in the system to the critical damping. Most of the experimental modal reported that the modal damping in terms of non-dimensional critical damping ratio expressed as a percentage [Formenti (1999); Gade, Herlufsen and Konstantin-Hansen (2002)]. In fact, most structures have critical damping values in the range of 0 to 10%, with values of 1 to 5% as the typical range [MSC.NASTRAN (2005)]. Zero damping ratio indicates that the mode is undamped. Damping ratio of one represents the critically damped mode. The result of the frequency response finite element analysis with zero Hz i.e. the maximum principal stresses distribution of the cylinder block is presented in Fig. 7 respectively. From the results, the maximum and minimum principal stresses of 380.0 MPa and -77.5 MPa for the Pseudo static analysis, and 380.0 MPa and -78.3 MPa for the frequency response analysis for zero Hz were obtained respectively. These two maximum principal stresses contour plots are almost identical.

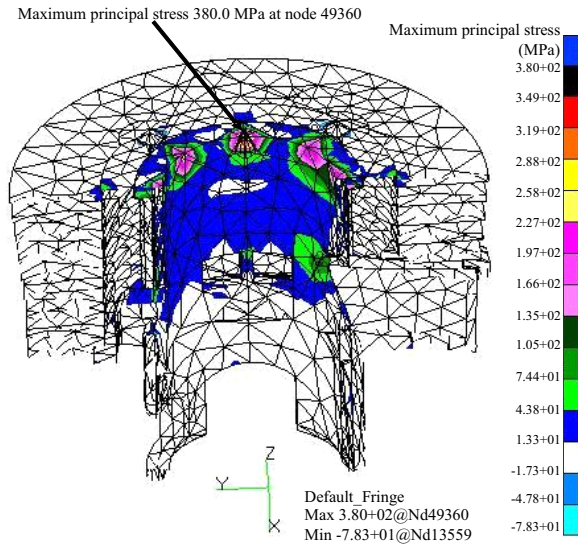


Figure 6: Maximum principal stresses distribution for the Pseudo-static linear analysis

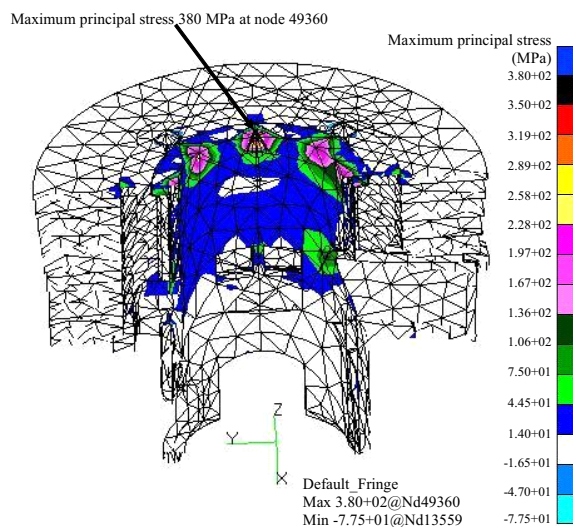


Figure 7: Maximum principal stresses distribution for the frequency response analysis with zero Hz

The variation of the maximum principal stresses with the frequency is shown in Fig. 8. It can be seen that the maximum principal stress varies with the higher frequencies. This variation is due to the dynamic influences of the first mode shape. It is also observed that the maximum principal stress occurs at a frequency of 32 Hz. The maximum principal stresses of the cylinder block for 32 Hz is presented in Fig. 9. From the results, the maximum and minimum principal stresses of

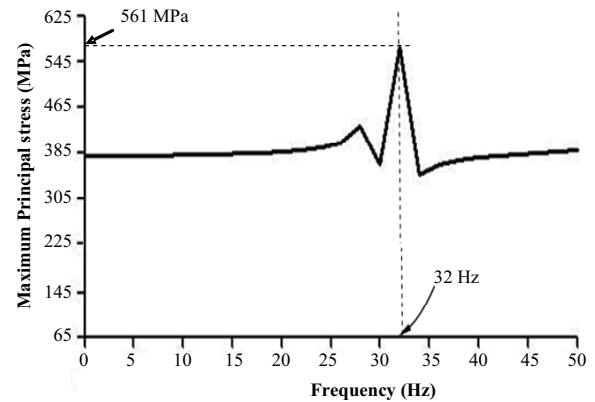


Figure 8: Maximum principal stresses plotted against frequency

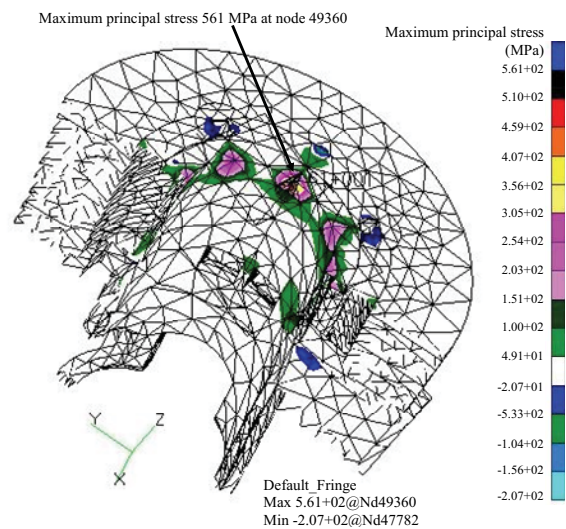


Figure 9: Maximum principal stresses contour for the frequency response analysis with 32 Hz

561.0 MPa and -207.0 MPa were obtained at node 49360 and 47782 respectively.

3.2 Loading Information

Several types of the variable amplitude loading histories were selected from the SAE and ASTM profiles for the FE based fatigue analysis. It is important to emphasize that these sequences are not indented to represent standard loading spectra in the same way that Carlos or Falstaf [MSC.FATIGUE (2005)] was performed. However, they do contain many features which are typical of the automotive industries applications, and therefore, are useful in the evaluation of the

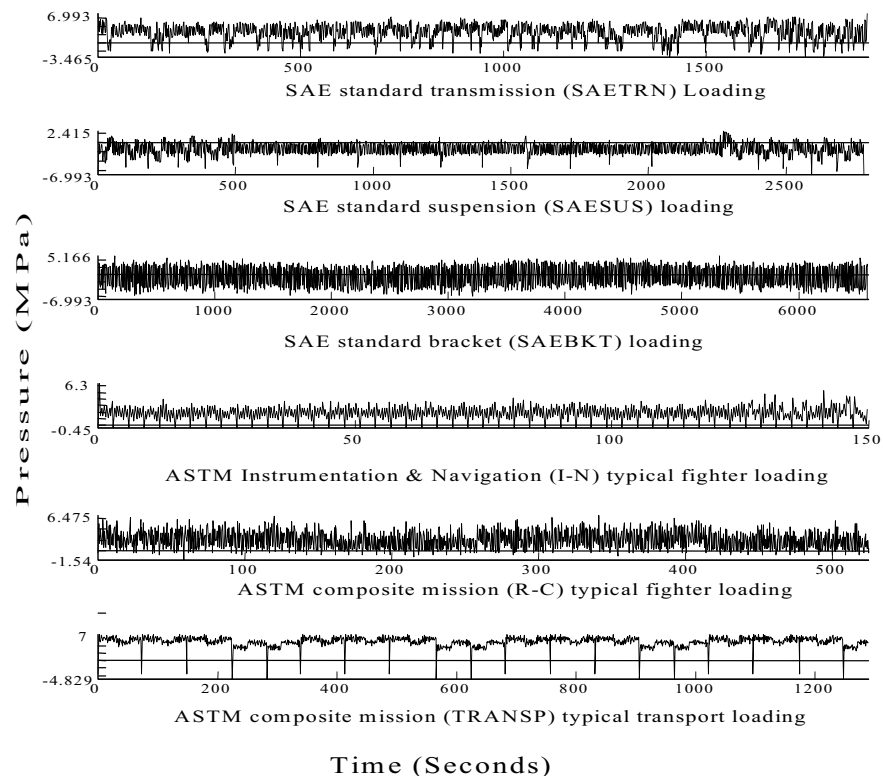


Figure 10: Different time loading histories

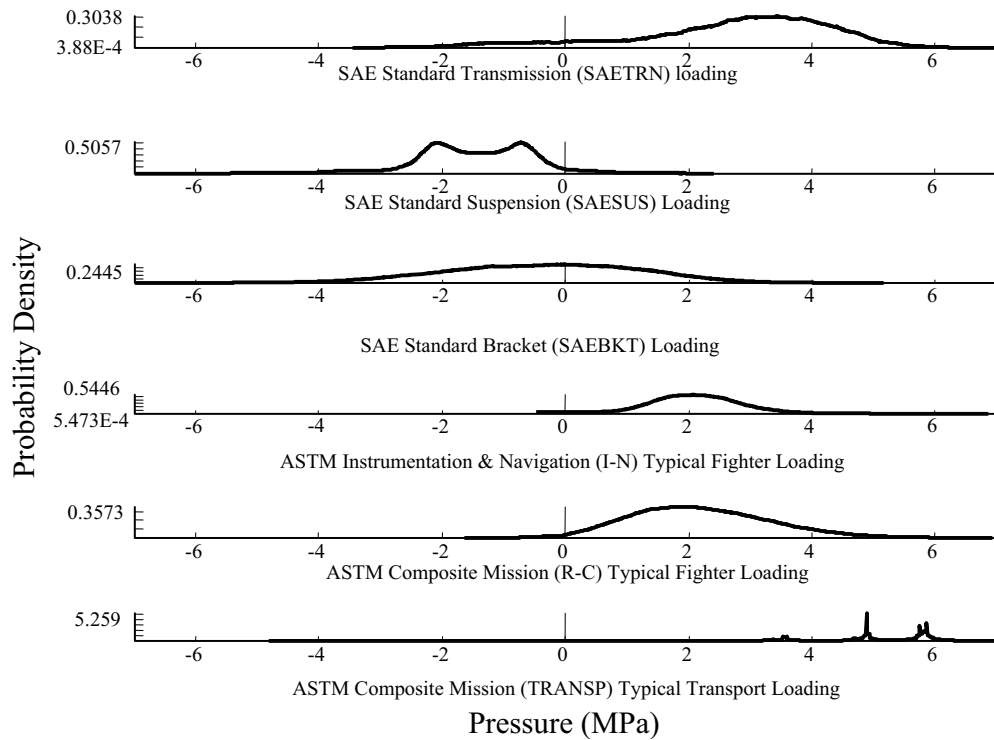


Figure 11: Power spectral densities response

life estimation methods. The component was loaded with three random time histories, corresponding to typical histories for the transmission, suspension and bracket components at different load levels. The first load history has a predominantly tensile (positive) mean which reflects sudden changes in mean, which is referred to as the transmission history. The second load history has a predominantly compressive (negative) mean, which is referred as suspension history. The third load history representing a vibration with nearly zero mean loads, which is referred as the bracket history. The detailed information about these histories can be referred in the literature [Tucker and Bussa (1977); Chang and Hudson (1981)]. These histories were scaled to two peak strain levels and used as full-length histories. In addition, a random history including many spikes was selected for the simulation of spike removal. The variable amplitude load-time histories are shown in Fig. 10 and the corresponding power spectral densities responses are also shown in Fig. 11. The terms of SAETRN, SAESUS, and SAEBKT represent the load-time history for the transmission, suspension, and bracket respectively. The considered load-time histories are based on the SAE's profile. In addition, I-N, R-C, and TRANSP are representing the ASTM instrumentation and navigation typical fighter, ASTM composite mission typical fighter loading history, and ASTM composite mission typical transport loading history respectively [Tucker and Bussa (1977)]. The abscissa is the time, in seconds.

3.3 Fatigue Life Prediction Analysis

The results of the fatigue life contour for the SAETRN loading histories at most critical locations for Pseudo-static analysis and frequency response approach with 32 Hz are shown in Fig. 12 and Fig. 13 respectively. The minimum life prediction for Pseudo-static analysis and frequency response approach with 32 Hz are obtained $10^{7.67}$ and $10^{9.44}$ seconds respectively. It would be expected that the condition of lower stress would correspond to longer life and vice versa. However, the results indicates the opposite because the frequency resolution of the transfer function are

selected the small value then the result show the non-conservative prediction. From Fig. 12 and Fig. 13, it can be seen that the fatigue life contours are different and most damage was found at frequency of 32 Hz.

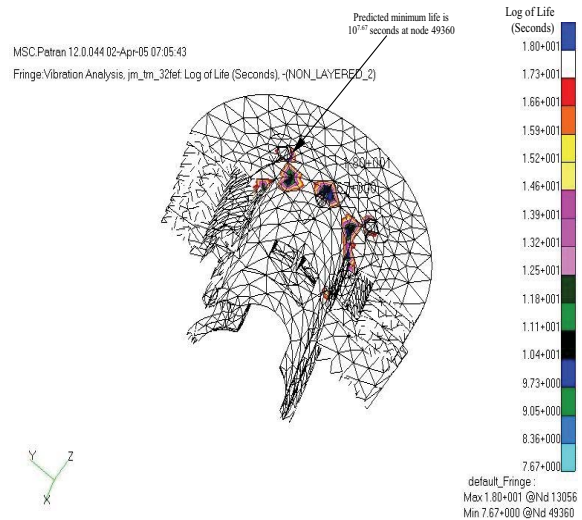


Figure 12: Predicted fatigue life contours plotted using the Pseudo-static method

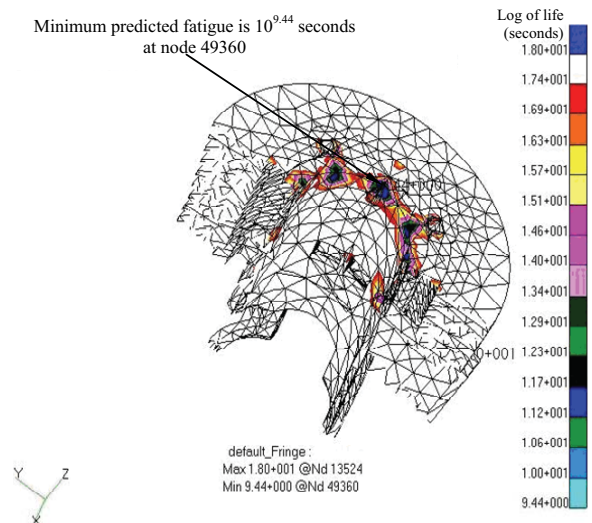


Figure 13: Predicted fatigue life contours plotted using the frequency response analysis for 32 Hz

For the purpose of validation, the predicted life listed below will be taken to be the definitive answers. Table 1 shows the correlation between the frequency response analysis method and the conventional time domain Pseudo-static approach.

Table 1: Predicted life in seconds between two approaches at most critical location (node 50420)

Loading Conditions	Predicted fatigue life in seconds at critical location (node 50420)	
	Pseudo-static approach (seconds)	Vibration analysis (seconds)
SAETRN	1.14×10^8	2.10×10^7
SAESUS	6.34×10^9	8.74×10^{10}
SAEBKT	7.56×10^7	4.06×10^8
ASTM I-N	3.02×10^9	2.30×10^8
ASTM R-C	1.27×10^6	6.02×10^7
ASTM TRANSP	1.15×10^7	2.27×10^9

The predicted fatigue life on log-log coordinates using the Pseudo-static and frequency response analysis is presented in Fig. 14. The solid straight line in Fig. 14 represents the perfect correlation between the pseudo-static and frequency response analysis results i.e. one to one correspondence if the vibration fatigue predicted life exactly equivalent to the pseudo-static predicted life. The two straight dotted lines represent a three times factor indicating a goodness band. Data points that fall above the solid line represent non-conservative estimates, while points below the solid line represent conservative predictions in comparison to the pseudo-static time domain results. It can be seen that the predicted fatigue life obtained from the vibration analysis using narrow band approach is in good agreement with the predicted life using the Pseudo-static time domain approach. Most of the predicted data falling well within the scatter band, which is shown in Fig. 14. It can be also seen that the frequency response analysis method tended to be conservative due to the data points concentrates on the lower band i.e. with the solid line and the lower dotted line. This indicates that the predicted life using the frequency response approach was reasonable and acceptable.

3.4 Nitriding Treatment

The free surface of a component is a common site for the initiation of fatigue crack. Therefore, the manner in which the surface is prepared during manufacturing of the component has a vital role in dictating the initiation life for the fatigue cracks. There exists a variety of surface treatment such as carburizing, nitriding, flame hardening, induction hardening etc, which are designed to impart high strength, wear resistance or corrosion resistance

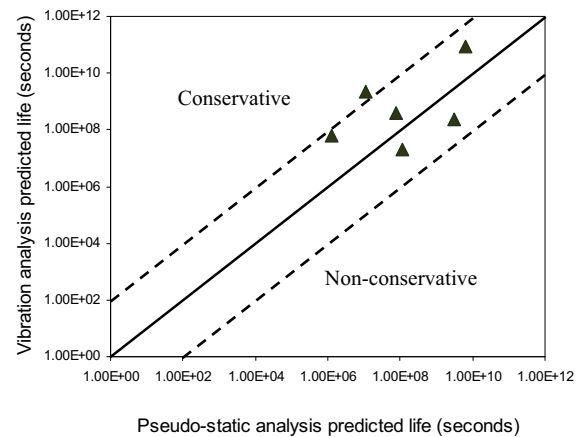


Figure 14: Correlation between the fatigue life between the Pseudo-static and frequency response analysis

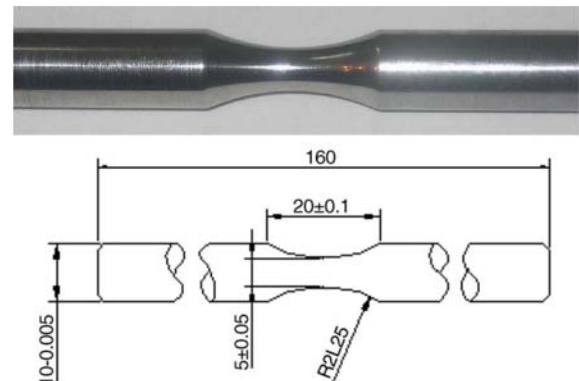


Figure 15: Typical specimen

locally in the near surface regions of the material. The nitriding was performed using a gas nitriding furnace at 550°C for 48 hours in ammonia atmosphere. At the end of the process, specimens were air cooled. Due to the process temperature was lower than the tempering temperature of the ma-

material, there was no tempering effect during the nitriding process so the microstructure of the material and its hardness remained unchanged during the process.

Fig. 15 shows a typical specimen for nitrided treatment. Fig. 16 shows optical micrograph of a typical hardened specimen. It is observed that the microstructure of the hardened specimens becomes homogeneous. However, it contains some retained austenite and white alloy carbides in a matrix of tempered martensite. Fig. 17 shows the micrographs of typical nitrided specimen. A thin compound (white) layer as well as a relatively thick diffusion layer was formed on the surface of the specimen. According to the Fig. 17, the diffusion layer formed a continuous matrix of alloy nitrides, which surrounds martensite grains and precipitated at the grain boundaries. It becomes obvious that this brittle hard matrix can be prone to initiation and consequently propagation of the fatigue cracks. In addition, due to the increase in surface roughness after the nitriding, fatigue cracks will appear more rapidly than would be the case on polished specimens. It is also clear that the nitriding has changed microstructure homogeneity.

According to the scanning electron microscope (SEM) investigations, it is shown in Fig. 18 that nitriding surface treatments roughen the surface of specimens. It is obvious from Fig. 18 that the outer layer of specimens subjected to nitriding treatment, has a porous structure, which is of a columnar morphology. In nitrided specimens the large pores are created near the intersection of compound layer and diffusion layer. Therefore, due to the roughness, the time needed for crack initiation stage is short. Cracks easily initiate from the rough outer surface and may then propagate through the porous structure at a high to reach critical dimensions sufficient to cause final fracture. Due to the location of large pores and the less rough outer surface in nitrided specimens, the crack initiation stages take more time. After performed the nitriding process, the specimen was polished to improve the surface roughness.

When the nitriding process is properly done, then

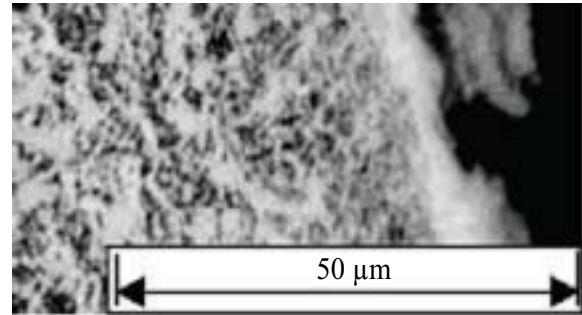


Figure 16: Optical micrograph of typical hardened specimen

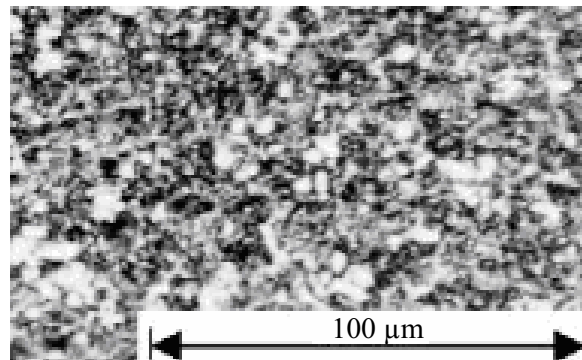


Figure 17: Micrograph of typical nitrided specimen

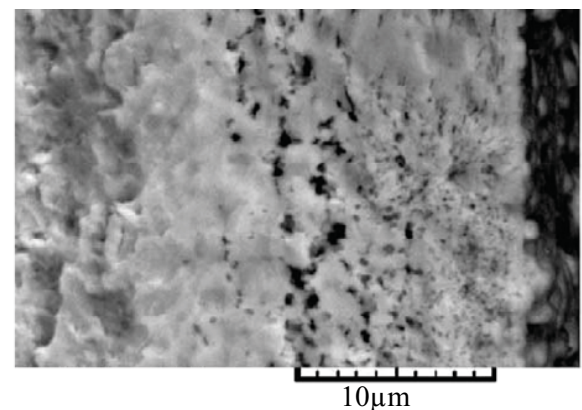


Figure 18: SEM micrograph of nitrided specimen

it leaves components with a surface skin that is hard and in compression. The compression residual stress can reach the yield strength of the nitrided skin. It is very effectively prevents the formation and growth of the cracks and thus permits to realize the gain in fatigue strength that would expect from the increased hardness. The nitrid-

Table 2: Effect of nitriding treatment at different loading conditions for polished components

Loading Conditions	Predicted fatigue life at most critical location	
	Nitrided (seconds)	Untreated (seconds)
SAETRN	4.52×10^{10}	2.10×10^7
SAESUS	3.41×10^{16}	8.74×10^{10}
SAEBKT	8.08×10^{12}	4.06×10^8
I-N	6.35×10^{12}	2.30×10^8
R-C	7.21×10^{10}	1.83×10^7
TRANSP	2.40×10^{14}	2.27×10^9

ing process has the combined effect of producing a higher strength on the surface as well as causing the volumetric changes due to phase transformation that produce residual compressive surface stresses.

The algorithm for calculating the high cycle fatigue contributions is based on the consideration of the magnitude of each cycle and the part of the life curve used to calculate damage for that cycle. The reasoning behind this logic is that the structures experiencing low-cycle fatigue problems are solved by increasing the strength of the material and by carrying out surface treatments. Surface treatments that introduce stresses usually compressive into the surface of a component have a significant effect upon fatigue life. Correction factors for a range of surface treatments are therefore available in Ref. [MSC.FATIGUE (2005)].

The effect of nitriding treatment upon the fatigue life of component subjected to variable amplitude loading conditions for cylinder block of free piston engine is investigated in this section. The polished aluminum alloy AA6061-T6 is considered in this study. The contributions of nitriding treatment on the fatigue life at different loading conditions using narrow band frequency response method at critical location are tabulated in Table 2. Nitriding that produce compressive residual surface stresses are useful. This treatment causes the maximum tensile stress to occur below the surface. Nitriding is increase the endurance limit. It is very beneficial for fatigue strength. This process has the combined effect of producing a higher strength material on the surface as well as causing volumetric changes, which produce residual compressive surface stresses. The

great improvement in fatigue life is due primarily to the residual compressive stresses.

From Table 2, it is observed that the fatigue life for nitriding treatments is surprisingly increases than untreated conditions due to the compressive residual stresses produce on the surface of the component. Fig. 19 shows that the effect of nitriding processes at different loading conditions and polished specimen. It is clearly seen that nitrided processes are surprisingly increases the fatigue life at critical location. It can also be seen that SAESUS and SAETRN loading conditions found the highest and lowest lives of the cylinder block respectively.

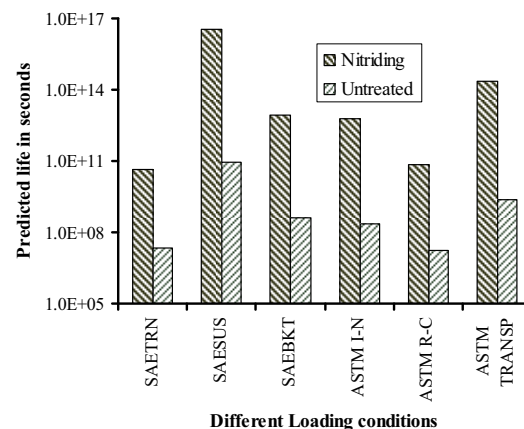


Figure 19: Effect of nitriding processes at different loading conditions for polished surface

4 Conclusions

This paper conveys important findings on the influence of the nitriding surface treatment process parameter on the fatigue lives. The vibration fatigue analysis technique has presented when the

random loading are categorized using PSD functions. Narrow band frequency response analysis has applied to a typical cylinder block for the new two-stroke free piston linear engine. According to the results, it can be concluded that the polished and nitriding combinations found the great influences on the fatigue life improvement. Nitriding treatment is to produce compressive forces in the outer layers of the component. In addition, the vibration fatigue analysis can improve understanding of the system behaviors in terms of frequency characteristics of both structures and loads and their couplings. The proposed approach can be used for durability assessment of a prototype engine with actual service conditions in the early developing stage.

Acknowledgement: The authors would like to thanks to Malaysia Government especially Ministry of Science, Technology and Environment under IRPA project (IRPA Project no. 03-02-02-0056 Pr0025/04-03) for providing financial support.

References

- Anthes, R.J.** (1997). Modified rainflow counting keeping the load sequences. *International Journal of Fatigue*, 19(7): 529-35.
- Bell, T.; Mao, K.; Sun, Y.** (1998): Surface engineering design: modeling surface engineering systems for improved tribological performance. *Surface and Coating Technology*, 108-109: 360-368.
- Bendat, J.S.** (1964): *Probability functions for random responses*, NASA report on Contract NASA-5-4590.
- Bishop, N.W.M.; Sherratt, F.** (2000): *Finite element based fatigue calculations*. UK: NAFEMS Ltd.
- Boms, R.; Whitacre, D.** (2005): Optimization design of aluminum suspension components using an integrated approach. *SAE 95M-2*.
- Chang, J.B.; Hudson, C.M.** (1981): *Methods and models for predicting fatigue crack under random loading*. USA: American Society for Testing and Materials.
- Felippa, C.A.** (2001): *Advanced finite element methods*. Department of Aerospace Engineering Sciences, University of Colorado.
- Formenti, D.** (1999): The relationship between % of critical and actual damping in a structure. *Sound and Vibrations*, 33: 14-18.
- Gade, S.; Herlufsen, H.; Konstantin-Hansen, H.** (2002): How to determine the modal parameters of simple structures. *Sound and Vibrations*, 36: 72-73.
- Khosrovaneh, A.K.; Downing, N.E.** (1990): Fatigue loading history reconstruction based on rainflow technique. *International Journal of Fatigue*, 12(2): 90-106.
- MSC.FATIGUE.** (2005): *User's guide*. USA: MSC.Software Corporation.
- MSC.Nastran** (2005): *User's guide, Basic dynamic analysis*, MSC.Nastran Version 68, MSC.Software Corporation, USA.
- Novovic, D.; Dewes, R. C.; Aspinwall, D. K.; Voice, W.; Bowen, P.** (2004): The effect of machined topology and integrity on fatigue life. *International Journal of Machine Tools & Manufacture*, 44: 125-134.
- Rahman, M.M.; Ariffin, A.K.** (2006): Effects of surface finish and treatment on the fatigue behaviour of vibrating cylinder block using frequency response approach. *An International Journal of Applied Physics and Engineering*, 7(3): 352-360.
- Rahman, M.M.** (2007): *Finite element based durability assessment for a new free piston linear engine*. PhD Thesis. Universiti Kebangsaan Malaysia.
- Rice, S.O.** (1954): *Mathematical analysis of random noise*. Selected papers on Noise and Stochastic Processes. New York: Dover.
- Schaeffer, H.G.** (2001): *MSC.NASTRAN Primer for Linear Analysis*. MSC.Software Corporation, USA.
- Torres, M.A.S.; Voorwald, H.J.C.** (2002): An evaluation of shot peening, residual stress and stress relaxation on the fatigue life of AISI 4340 steel. *International Journal of Fatigue*, 24: 877-886.

Tucker, L.; Bussa, S. (1977): *The SAE cumulative fatigue damage test program: fatigue under complex loading, analysis and experiments*. R.M. Wetzel, ed., Society of Automotive Engineers, USA, AE-6: 1-54.

Vissutipitukul, P.; Aizawa, T. (2005): Wear of plasma nitrided aluminum alloys. *Wear*, 259: 482-489.

